

Studies of the positron lifetime and Doppler-broadened annihilation radiation of polypropylene–polystyrene alloys

G. Dlubek^{a,b,*}, M.A. Alam^a

^a*H.H. Wills Physics Laboratory, University of Bristol, Tyndal Avenue, Bristol BS8 1TL, UK*

^b*ITA Institut für Innovative Technologien GmbH Köthen, Aussenstelle Halle, Wiesenring 4, D-06120 Lieskau (bei Halle/S.), Germany*

Received 2 January 2002; accepted 15 March 2002

Abstract

Positron annihilation lifetime spectroscopy and Doppler-broadened annihilation radiation (DBAR) experiments were performed on polypropylene–polystyrene (PP–PS) alloys (0–100% styrene) prepared by in situ polymerisation of styrene in a PP host matrix. The mean size of free-volume holes estimated from the *ortho*-positronium lifetime τ_3 shows a continuous decrease from 0.119 nm³ in PP to 0.095 nm³ in PS. The intensity of the *o*-Ps component, I_3 , the average positron lifetime τ_{av} , the curve-shape parameter S and the peak height H of the DBAR spectra increase linearly with the styrene concentration. This is attributed to a linear superposition of the Ps yields of PP and PS in the PP–PS alloys. The DBAR spectra were fitted by a sum of three Gaussians, the narrowest of them is attributed to self-annihilation of *para*-positronium confined within holes. After its subtraction, a ‘broad component’ is obtained which represents the momentum distribution of electrons bound to molecules. Its normalised peak height does not show any change with the composition which reflects the fact that both constituents of the PP–PS alloys contain only hydrogen and carbon atoms in their chemical units. Immersing of PP into styrene liquid leads to a very pronounced increases in the lifetime parameters which is attributed to the plasticisation of PP. © 2002 Elsevier Science Ltd. All rights reserved.

Keywords: Polypropylene; Polystyrene; Polymer alloy

1. Introduction

Physical combination of two or more synthetic polymers is one of the widely used methods for producing new materials interesting both from practical and scientific points of view [1]. The main ways for realising such combination are the mixing of polymers during extrusion from the melt (formation of polymer blends) or the mixing of different monomers and polymerisation of the mixture (formation of copolymers). A special way for combining different polymers is the solid-phase modification. A monomer is allowed to diffuse into a host polymer followed by its polymerisation inside the solid matrix. The system formed in this way may be called a polymer ‘alloy’. One of such interesting systems is the polypropylene–polystyrene alloy which is prepared by diffusion of styrene into the amorphous phase of semi-crystalline polypropylene (PP). The system shows modified

structure, high dispersion of polystyrene (PS) and interesting mechanical properties [2,3]. Investigation of its structure and properties are therefore of high interest.

In this paper, we utilise measurements of the positron annihilation lifetime spectrum and the Doppler-broadened annihilation radiation (DBAR) [4] in order to study structural aspects of the PP–PS alloy system on a sub-microscopic scale over a large range of compositions together with the boundary polymers PP ($[-\text{CH}_2-\text{CH}(\text{CH}_3)-]_n$) and PS ($[-\text{CH}_2-\text{CH}(\text{C}_6\text{H}_5)-]_n$). The positron lifetime technique has found increasing interest and growing application in the studies of polymeric materials in recent years [5–9]. The reason for this is that it provides a unique probe for sub-nanometre local free (empty) volume holes in amorphous polymers that arise from their structural disorder. Such holes play a crucial role in determining a variety of properties of polymers, e.g. in the permeation of gas and liquid through such materials, changes in their behaviour under pressure, temperature and under the influence of plasticisers and in their general mechanical and rheological properties [10].

In addition to the lifetime experiments, we measure the Doppler-broadened annihilation energy line. The annihilation

* Corresponding author. Address: ITA Institut für Innovative Technologien GmbH Köthen, Aussenstelle Halle, Wiesenring 4, D-06120 Lieskau (bei Halle/S.), Germany. Tel.: +49-345-5512-902; fax: +49-40-360-3241-463.

E-mail address: gdlubek@aol.com (G. Dlubek).

energy line reflects the momentum distribution of the annihilating particles and contains, in its ‘narrow component’, also information on the hole size [4]. From a three-Gaussian fit of the DBAR spectra, we attempt to separate and subtract the narrow component from the total curve. The interest in the behaviour of the remaining ‘broad component’ stems from the fact that this contains information about the electrons bound to molecules [4] and reflects the electronic configuration of atoms and molecules forming the polymer alloy [11,12].

2. Experimental details

2.1. Samples and experiments

The specimens under investigation were prepared by sorption of gassy styrene into native powder of isotactical PP at 90 °C. The polymerisation was performed at 90 °C using dibenzol peroxyde as catalyst. Plates of the alloy containing finally between 19.3 and 59.3 wt% of PS were pressed at a temperature of 150 °C. (For more details of material preparation and characterisation, see Ref. [3]). As boundary systems semicrystalline PP (crystallinity ~50% from differential scanning calorimetry) and amorphous PS were studied.

The positron lifetime experiments were carried out at room temperature using a fast–fast coincidence system [4] with a time resolution of 235 ps (full width at half maximum, FWHM, of a Gaussian resolution function) and a channel width of 12.5 ps. The specimens were platelets of 8 × 8 mm² in area and 1.5 mm in thickness. For each experiment, two identical samples were sandwiched around a 5 × 10⁶ Bq positron source (²²Na), prepared by evaporating carrier-free ²²NaCl solution onto a Kapton foil of 8 μm thickness. Well-annealed aluminium platelets ($\tau = 162$ ps) were studied as a reference material for estimating the resolution FWHM and the positron source correction. For each of the specimens, 36 measurements each lasting 1200 s, were accumulated. Each 1200 s spectrum was inspected for possible time-zero drifts and only those spectra with a time-zero difference ≤ 1 channel were summed together to a final spectrum containing a high total number of ~25 × 10⁶ coincidence counts. For the final spectrum analysis, the counts in four consecutive channels were summed to improve statistics.

The momentum distributions were obtained via the Doppler broadened annihilation energy lines [4] measured by a high resolution intrinsic Ge detector system with an operational resolution of ~1.3 keV at the photo peak. The channel width was 0.123 keV. Six measurements, each lasting 2 h, were performed for each of the specimens. Following a preliminary inspection, the counts of those spectra for which various calculated lineshape parameters were within the estimated statistical accuracy of the experiments were summed to a final spectrum which contained a total number of ~10 × 10⁶ counts.

2.2. Data analysis

For a preliminary assessment of the lifetime spectra, we carried out data fitting using both discrete-component analysis (using routine LIFSPECFIT [13]) and continuous distribution (using the routine MELT). MELT [14] inverts the lifetime spectrum into a continuous lifetime distribution $I(\tau)$ using a quantified maximum entropy method. The lifetime distributions obtained for the PP–PS alloys exhibit three well-separated peaks with mass centres at $\tau_1 \sim 200$ ps, $\tau_2 \sim 420$ ps, and $\tau_3 = 1970$ ps (PS) to 2225 ps (PP). In molecular materials, the positron preferentially forms and annihilates from a bound state called positronium (Ps). The Ps forms either in the *para* (anti-parallel electron and positron spins: *p*-Ps) or in the *ortho* (parallel electron and positron spins: *o*-Ps) positronium states with a relative abundance of 1:3 [4]. The shortest two lifetimes above are attributed to *p*-Ps and free positron (not Ps) annihilation. In vacuum, a *p*-Ps has a lifetime 125 ps and annihilates via 2 γ -photons while an *o*-Ps lives 142 ns and annihilates via 3- γ . When within the free volume in polymers, the *o*-Ps has a finite probability of annihilating with an electron other than its bound partner (and of opposite spin) during the numerous collisions that it undergoes with the molecules of the surrounding walls, a process generally termed as the ‘pick-off’. The result is a drastically reduced *o*-Ps lifetime compared to its vacuum value and its annihilation in 2- γ . The *o*-Ps pick-off lifetime depends on the number of collisions with the surrounding walls and this lifetime sensitively mirrors the size and any variation of local free volumes (holes) [5–9].

For the final analysis of lifetime spectra, we used the routine LIFSPECFIT [13] which delivered discrete lifetime parameters with higher statistical accuracy than those obtained from MELT. In this (conventional) analysis, it is assumed that the positron lifetime spectrum can be described by a sum of (in our case three) discrete exponentials

$$s(t) = \sum (I_i/\tau_i)\exp[-(t/\tau_i)], \quad (1)$$

each having a characteristic positron lifetime of τ_i with a relative intensity of I_i , $\sum I_i = 1$. Following the subtraction of source annihilation components (380 ps/4%-NaCl and Kapton cover, and 2500 ps/0.4%-surface effects), the routine employs a non-linear least squares fit to estimate the parameters τ_i and I_i , the background per channel, the time-zero of the spectrum and the (Gaussian) resolution width. The lifetime τ_3 represents the weighted average of *o*-Ps annihilations from amorphous and possibly from the crystalline phases. We assessed the potential errors associated with combining the possible two *o*-Ps lifetimes (from amorphous and crystalline regions) into a single τ_3 by performing four term fits of the lifetime spectra. Our conclusion was that the *o*-Ps annihilations from holes in the amorphous phase dominates τ_3 , a result also obtained in Ref. [12] for similar materials. The lifetime τ_3 , its intensity I_3 and the

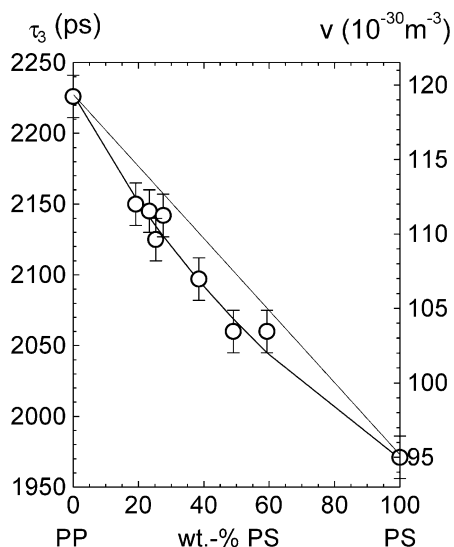


Fig. 1. The *o*-Ps lifetime τ_3 and the hole volume v calculated from τ_3 as a function of the PS content in PP-PS alloys. The curve represents a least-squares fit of Eq. (4) to the data points.

average positron lifetime τ_{av} estimated via $\tau_{av} = \sum I_i \tau_i$ are shown in Figs. 1 and 2.

The DBAR spectra were analysed by using the program ACARFIT of the data-processing system PATFIT-88 [15] and assuming that the experimental DBAR energy spectra consist of a sum of three equi-centred Gaussians [12],

$$F(E) = \sum J_i [1/(\sigma_i(2\pi)^{0.5})] \exp[-(E - E_0)^2/2\sigma_i^2], \quad (2)$$

$(i = 1, \dots, 3).$

J_i and σ_i denote the intensity and the standard deviation of

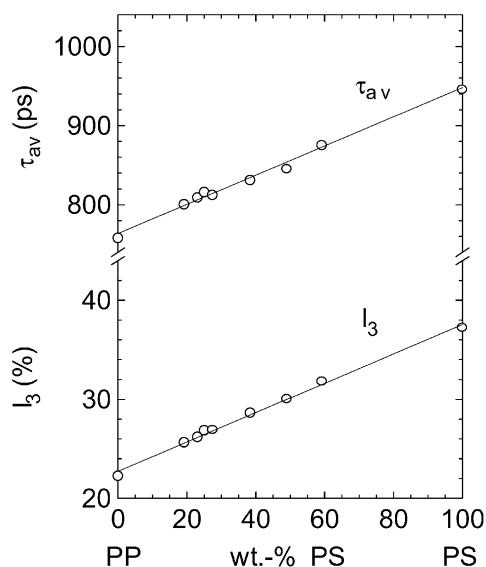


Fig. 2. The average positron lifetime τ_{av} and the intensity I_3 of the *o*-Ps component as a function of the PS content in PP-PS alloys. The straight line through the I_3 data (empty symbols) represents a least-squares fit of Eq. (5) to the experiments.

the *i*th Gaussian component, respectively, E is the energy of an individual γ and $E_0 = 511$ keV. The intensities are normalised as $J_1 + J_2 + J_3 = 1$. If we assume that the DBAR resolution may be expressed by a Gaussian with a half width at full maximum of $\text{FWHM}_r = 1.3$ keV, the deconvoluted DBAR spectra consist of a sum of Gaussians the standard deviation of which are given by $(\sigma_i^2 - \sigma_r^2)^{0.5}$, $\sigma_r = \text{FWHM}_r/2(2 \ln 2)^{0.5}$.

As a first step, the spectra were symmetrised by subtracting a non-linear background function (see Ref. [4], p. 44) fitted to the tail regions on the left and right of the Doppler peak using the routine SPARAM [16]. DBAR spectra treated in this way still exhibit a small anisotropy (Fig. 3) which results in a large variance of about 50 when fitting Gaussians. As discussed in our previous paper [12], we tried to overcome this problem by performing two further fits separately on the left (peak - 30 to peak + 10 channels) and right (peak - 10 to peak + 30 channels) hand sides of the spectra. This improves the variance of the fit to about 4, which is adequate considering that each DBAR spectrum contains 10^7 counts. The parameters obtained by the three different fitting methods agree except for a small systematic shift.

An example of such a fit to a DBAR energy distribution for PS is shown in Fig. 3. The FWHM of the Gaussians, W_i , were calculated via $W_i = 2(2 \ln 2)^{0.5} \sigma_i^{1/2}$. All DBAR curves could be adequately fitted to three Gaussians: a wide Gaussian (a: $W_3 = 4.9$ – 5.1 keV) of low intensity ($J_3 = 4.3$ – 5.2%), a high intensity ($J_2 = 84.6$ – 89.0%) and medium width Gaussian (b: $W_2 = 2.58$ – 2.62 keV), and a narrow Gaussian (c: $W_1 = 1.50$ – 1.66 keV; $J_1 = 6.4$ – 12.0%).

3. Results and discussion

The *o*-Ps lifetime τ_3 , plotted in Fig. 1 as a function of the styrene content of the PP-PS alloy, shows a non-linear decrease from 2225 ps in PP to 1970 ps in PS. Our lifetimes

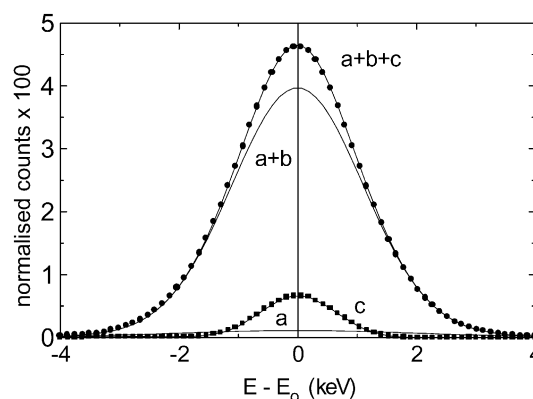


Fig. 3. Doppler-broadened annihilation line of polystyrene. Shown are the experimental data (circles) after subtraction of a non-linear background function and the three Gaussians *a*, *b* and *c*, their sum was fitted to the experimental data. The narrow component (squares) was obtained by subtraction $a + b$ from the experimental data points.

for the homopolymers agree well with those found in the literature for PP [17,18] and PS [19–23]. As mentioned previously, the *o*-Ps lifetime is related to the size of the holes where the Ps is confined and from which it annihilates. A simple model incorporating quantum mechanical and empirical arguments yields an analytical expression relating the hole (assumed spherical) radius (r) to the observed *o*-Ps pick-off lifetime [5–8] $\tau_3 = \tau_{po}$,

$$\tau_{po} = 0.5 \text{ ns} \left[1 - \frac{r}{r + \delta r} + \frac{1}{2\pi} \sin\left(\frac{2\pi r}{r + \delta r}\right) \right]^{-1}. \quad (3)$$

The factor of 0.5 ns is the inverse of the spin-averaged Ps annihilation rate [4], $\delta r = 1.66 \text{ \AA}$ represents the extent of the penetration of the Ps-wavefunction into the walls of the hole. The potential of the hole experienced by the Ps may be approximated by a square well potential of finite depth and radius r . Since the depth of the potential is unknown it is modelled by a square well potential of infinite depth and radius $r + \delta r$. $\delta r = 1.66 \text{ \AA}$ is obtained by fitting Eq. (3) to observed *o*-Ps lifetime of known mean hole radii in porous materials [5–8]. Eq. (3) allows the evaluation of an average hole radius r and hole volume $v = 4\pi r^3/3$ from the experimental *o*-Ps lifetime τ_3 . The averaging occurs over the size and shape distribution of the local free volumes.

As a result of the preparation of the PP–PS alloy, it is expected that the styrene monomers diffuse only into the amorphous phase of PP via the free-volume holes but not into the densely packed crystalline regions [2,3]. During the polymerisation, a fraction of styrene is grafted onto the PP macromolecules forming PS side chains, the remaining fraction forms free (not bound to PP) PS. The amorphous phase of the alloy then consists of three different types of macromolecules: unmodified PP chains, PP chains grafted with styrene, and free PS. From electron microscopy, it was found that the free PS is rather finely distributed with blurred phase boundaries to the PP regions due to the compatibilising effect of the PS-grafted to PP molecules. After melting and extrusion of our material, a slight phase separation with formation of small PS particles has been observed [3].

The right-hand scale of the y -axis in Fig. 1 shows the decreasing mean hole volume v (obtained from Eq. (3): $v = 4\pi r^3/3$) with increasing styrene content of the alloy from 0.119 to 0.095 nm³ (uncertainty: $\pm 0.002 \text{ nm}^3$). The radius decreases from $r = 0.305$ to 0.283 nm. The different hole sizes in PP and PS are compatible with their different glass transition temperatures T_g . Our materials have a T_g between 0 °C (PP) and 95 °C (PS). Thus our measuring temperature (25 °C) is well below the T_g of PS but somewhat above that of PP.

The decrease in the mean hole volume with increasing content of styrene can be interpreted as being due to a corresponding increase in the effective glass transition temperature of the copolymer. The time resolution of positron lifetime experiments is not high enough to ascertain

from the experiments whether two or possibly three glass transition temperatures may appear: one due to the PP phase, a second due to PP modified by grafted PS; and a third due to free PS. Moreover, a fraction of the PP in the alloys exists in the crystalline state. We have studied PP–PS alloys with different fractions of free and bound PS but the same total content of styrene. No clear changes in τ_3 or I_3 could be observed. The mean hole volume estimated from τ_3 represents an average over all chemical and structural phases present in the alloy. Owing to the higher Ps yield, the amorphous phase will dominate the experimental signal. The holes in the amorphous phase have a range of sizes and shapes. However, the hole sizes appearing within the PP and PS phases are too closely spaced to be resolved from our experiments.

To describe the *o*-Ps lifetime behaviour as a function of the alloy composition, we assume that τ_3 appears as the result of a weighted superposition of the *o*-Ps lifetimes from the PP crystals, $\tau_3^{\text{PP,c}}$, from PP amorphous phase, $\tau_3^{\text{PP,a}}$ and from the PS amorphous phase, $\tau_3^{\text{PS,a}}$,

$$\tau_3 = \{ [X_c^{\text{PP}} I_3^{\text{PP,c}} \tau_3^{\text{PP,c}} + (1 - X_c^{\text{PP}}) I_3^{\text{PP,a}} \tau_3^{\text{PP,a}}] (1 - c_{\text{PS}}) + c_{\text{PS}} I_3^{\text{PS,a}} \tau_3^{\text{PS,a}} \} / I_3, \quad (4)$$

with

$$I_3 = [X_c^{\text{PP}} I_3^{\text{PP,c}} + (1 - X_c^{\text{PP}}) I_3^{\text{PP,a}}] (1 - c_{\text{PS}}) + c_{\text{PS}} I_3^{\text{PS,a}} \quad (5)$$

Due to the very small mean Ps diffusion length in amorphous polymers of $\Lambda_{\text{Ps}} \approx 2 \text{ nm}$ [29], we expect that these linear relations are justified for the PP–PS alloys which exhibit, as mentioned previously, fairly distinctly separated microphases [3]. In the above equations, $X_c^{\text{PP}} = 0.5$ is the crystallinity of the PP phase and c_{PS} denotes the fraction of PS in the PP–PS alloy. $I_3^{\text{PP,c}}$, $I_3^{\text{PP,a}}$, and $I_3^{\text{PS,a}}$ are the intensities of the *o*-Ps lifetime component from the (100%) crystalline and (100%) amorphous phases of PP and from PS. The lifetime measurements of pure PS delivered $\tau_3^{\text{PS,a}} = 1970 \text{ ps}$ and $I_3^{\text{PS,a}} = 36.8\%$. From a least squares fit of Eqs. (4) and (5) to experimental values of τ_3 and I_3 (curve in Fig. 1 and straight lines in Fig. 2), we obtain $I_3^{\text{PP,c}} = (5 \pm 3)\%$, $I_3^{\text{PP,a}} = (39 \pm 3)\%$, and $\tau_3^{\text{PP,a}} = (2385 \pm 100) \text{ ps}$. In the fit $\tau_3^{\text{PP,c}}$ has been fixed to a value of 1000 ps in order to reduce the number of free fitting parameters. This lifetime was estimated from the empirical relation between the crystalline packing coefficient and the *o*-Ps lifetime in hydrocarbon crystals published by Lightbody et al. [24] and correspond to a packing coefficient of 0.72 which is typical for polymer crystals [25,26]. The results of the fit show that the *o*-Ps yield (I_3) of the amorphous phase of PP is almost the same as in PS. The small *o*-Ps yield estimated for crystalline PP is typical for polymer crystals [25–28]. $\tau_3^{\text{PP,a}} = 2385 \text{ ps}$ corresponds to a hole volume of $v = 0.135 \text{ nm}^3$. This correlates well with the hole volume in PS at a temperature of $T = T_g + 25 \text{ °C} = 120 \text{ °C}$, $v = 0.140 \text{ nm}^3$ [23].

We have also generated for the range of PP–PS alloys

lifetime spectra by composition weighted superposition of the spectra of the individual homopolymers. Analysis of these synthesised spectra provides almost the same τ_3 and I_3 values as those measured. This agreement justifies the use of the relations (4) and (5).

In Fig. 2, the behaviour of average positron lifetimes τ_{av} (empty circles) is plotted together with the intensity of the third lifetime component, I_3 . $\tau_{av} = \sum I_i \tau_i$ ($i = 1-3$) represents an integral parameter which does not depend on the particular model for describing the lifetime spectrum. Due to the large value of τ_3 , the average lifetime is dominated by the term $I_3 \tau_3$. Both τ_{av} and I_3 increase approximately linearly from PP to PS which may be attributed to a linear superposition of the *o*-Ps yields of PP and PS in the PP–PS alloy as it is assumed in Eq. (5).

We have also measured a PP specimen following its immersion in styrene monomer liquid at room temperature for a period of 5 days. From weight measurements, the styrene content was estimated to 27 wt%. The effect on the lifetime spectra was a dramatic increase in the annihilation parameters compared with PP: τ_3 from 2225 to 2802 ps; I_3 from 22.0 to 36.1%; and τ_{av} from 758 to 976 ps. We attribute this effect to a plasticisation of PP by styrene monomers. The increase in τ_3 corresponds to an increase in the apparent hole volume from 0.119 to 0.180 nm³. It is important to note that these lifetime parameters are distinctly larger than in the PP–PS alloy with the same styrene weight fraction. This observation opens the way for in situ investigations of the polymerisation process of styrene in solid PP. Such studies are currently in progress.

As has been mentioned previously, the DBAR spectra were fitted by a sum of three Gaussians (Fig. 3). Their FWHMs, W_i , plotted in Fig. 4, show no (W_2 and W_3) or only a weak (W_1) dependence on the composition of the copolymer. Such a behaviour, also observed in the tempera-

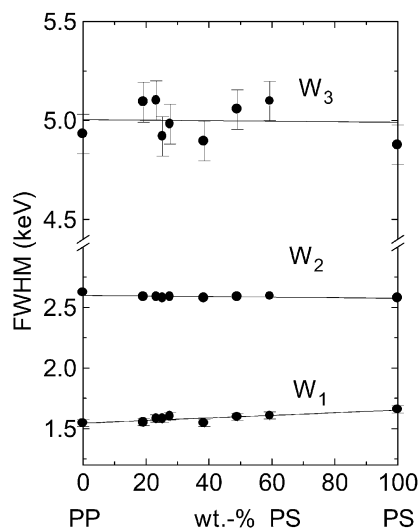


Fig. 4. Dependence of the FWHM W_i obtained from an unconstrained fit of a sum of three equi-centred Gaussians to the DBAR spectra as a function of the PS content in PP–PS alloys.

ture dependence of W_i for PE [11], can be considered as being typical for polymer alloys made from constituents containing only carbon and hydrogen atoms in their chemical units. The reason for this is discussed in detail in Ref. [12]. The DBAR spectra of polymers consist of components arising from the three basic annihilation channels: (i) free positron (e^+) annihilation, (ii) Ps pick-off annihilation (both occurs with electrons bound to molecules), and (iii) *p*-Ps self-annihilation. We attribute the broad curves to free positron and Ps pick-off annihilation with bound electrons, however, without attributing one of the broad Gaussians to a certain channel of annihilation. We only assume that a broad DBAR component, arising from the superposition of both broad Gaussians, describes well the integral effect of free positron and Ps (mainly *o*-Ps) pick-off annihilation. This broad DBAR component contains information about the electronic configurations of the molecules whose electrons take part in the annihilation process [12]. Owing to this, its shape may differ distinctly for polymers containing different chemical constituents.

The narrowest Gaussian is assumed to represent the so-called narrow component, that is the momentum distribution of the *p*-Ps decaying from a confined state inside the holes via self-annihilation [4]. The FWHM of the narrow component, $W_n = W_1$, reflects as consequence of the Heisenberg uncertainty principle, the localisation momentum of the *p*-Ps restricted within the holes and can be related to the extent of its localisation in a similar fashion to Eq. (3) [6],

$$W_n = \frac{1.66}{r + \delta r}. \quad (6)$$

Here, W_n is given in mrad (1 mrad in angular correlation of annihilation radiation curves corresponds to 0.2555588 keV in DBAR energy distribution) and r in nm, $\delta r = 0.166$ nm. Both Eqs. (3) and (6) depend exclusively on the size of the holes which confine the Ps and not on their chemical surroundings.

In Fig. 5, we plot the intensity of the narrow component of the DBAR distribution $I_n = J_1$ which is a useful indicator of the *p*-Ps yield $P_{p-Ps} = P/4$. Due to a small amount of *p*-Ps pick-off annihilation, I_n is slightly smaller than P_{p-Ps} : $I_n = P_{p-Ps} \eta \lambda_{p-Ps}^0 / (\eta \lambda_{p-Ps}^0 + \lambda_{po}) \approx 0.95 P_{p-Ps}$, where $\eta \approx 0.8$ denotes the Ps relaxation parameter, $\lambda_{po} \approx \tau_3^{-1} = (2 \text{ ns})^{-1}$ is the pick-off rate and $\lambda_{p-Ps}^0 = (125 \text{ ps})^{-1}$ [4]. P_{p-Ps} may also be estimated from lifetime experiments as the intensity of the *p*-Ps component, $P_{p-Ps} = I_1$, or from the *o*-Ps yield, $P_{p-Ps} = P_{o-Ps}/3 = I_3/3$ which is more accurate. As seen in Fig. 5, the experimental I_n values lie somewhat below $0.95 I_3/3$. In Fig. 5, we also present experimentally obtained values of W_n . These are compared with calculated values of W_n derived from Eq. (6) using hole radii estimated from measured *o*-Ps lifetime τ_3 . The values presented for W_n (cal) in Fig. 5 have been convoluted with the energy resolution function. Here, again we observe the trend of values derived from DBAR experiments lying below those derived from lifetime measurements. It may be due to physical

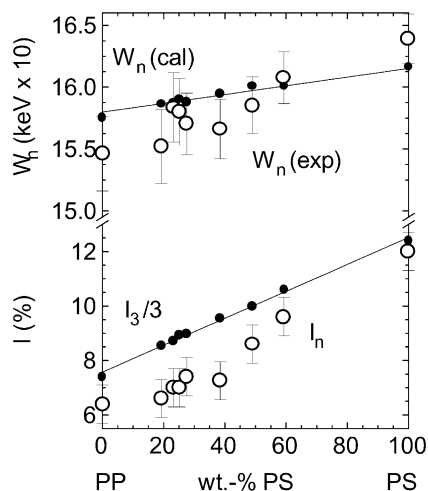


Fig. 5. Width W_n (exp) and relative intensity I_n of the narrow DBAR component in PS–PP alloys. W_n (cal) was calculated from the hole radius r (Eq. (6)) which was estimated via Eq. (3) from the value of τ_3 . I_3 is the intensity of the *o*-Ps lifetime component.

reasons discussed in detail by Mogensen ([4], p. 61 and 222). It may, however, just reflect an underestimation of the *p*-Ps self-annihilation by the narrowest Gaussian. Nevertheless, both W_n (exp) and I_n follow the trends estimated from the lifetime spectra. This we consider as an indication that the narrowest Gaussian of the DBAR distribution provides a realistic description of the self-annihilation of *p*-Ps within the holes in these samples.

If we accept this conclusion, we may now subtract the narrow Gaussian from the total DBAR curve in order to obtain the DBAR momentum distribution of bound electrons. As a measure of the DBAR curve shape, we have plotted in Fig. 6 the normalised peak-heights H and H_b (see below), together with conventional curve-shape

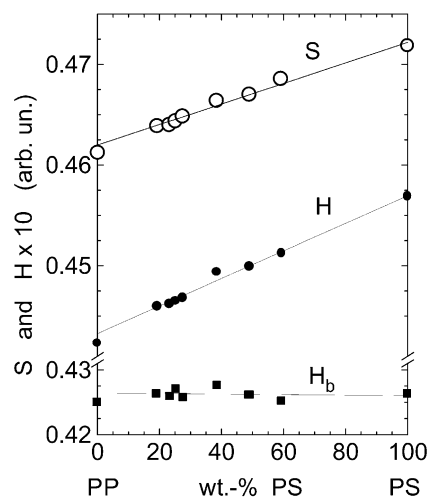


Fig. 6. DBAR curve-shape parameter S and peak height H normalised to the area below the total DBAR curve in the PP–PS alloys. The parameter H_b represents the peak height of the broad DBAR component renormalised to the area below it.

parameter S . S is calculated by summing-up the counts in the central region of the photo peak and dividing this sum by the total number of counts in the spectrum. The peak height $H = F(E_0)$ (Eq. (2)) is a similar parameter as S [4]; it is obtained in our case from the fit of the three Gaussians to the experimental spectrum and normalisation to the area below the total curve. S and H are integral parameters, their behaviour correlates that of τ_{av} . As we discussed in detail in Ref. [11], the average lifetime is dominated by the *o*-Ps yield ($I_3\tau_3$), while the variation in H and S are due to changes in the intensity of the *p*-Ps self-annihilation (I_n). H_b is the peak height of the curve consisting of the two broad Gaussians renormalised to the area below the both. It is a parameter reflecting the shape of the distribution which is due to free positron and *o*-Ps pick-off annihilation with bound electrons. The perfect constancy of H_b indicates that the chemical nature of the atoms or molecules does not change in the PP–PS alloys. The alloys consist only of hydrogen (electronic configuration $1s^1$) and carbon atoms ($2s^22p^2$). A change in the number of carbon and hydrogen atoms per chemical repeating unit ($[-CH_2-CH(CH_3)-]$ in PP and $[-CH_2-CH(C_6H_5)-]$ in PS) is obviously without effect on H_b . Contrary to that, we observed a strong decrease of H_b from a value of 0.043 for PE ($[-CH_2-CH_2-]_n$) via 0.040 for polyoxymethylene (POM, $[-CH_2-O-]_n$) to 0.0365 for PTFE ($[-CF_2-CF_2-]_n$) [12]. This is due to the substitution of CH_2 by oxygen ($2s^22p^4$) and hydrogen by fluorine ($2s^22p^5$). Our experience with the parameter H_b indicate clearly that the broad component in the DBAR spectra shows an enhanced sensitivity to the presence and number densities of various types of atoms in the material and in this way on the chemistry of polymer but show little or no correlation to Ps yield and the spatial structures of the free-volume holes. This conclusion is confirmed by our experiments published in Ref. [12].

4. Conclusions

The *o*-Ps lifetime τ_3 and the size of local free volumes (holes) calculated from its value shows a continuous decrease from PP to PS in PP–PS alloys prepared by post-polymerisation of styrene inside a PP host matrix. The behaviour of the hole volume may be described as an average over the hole volumes of the amorphous phases of PP and PS weighted with the *o*-Ps yield and the weight fraction of the constituents of the PP–PS alloy. Due to the occurrence of a fraction of crystalline PP, the estimated hole volume is slightly smaller than the true value. The different mean hole volumes in the boundary systems PP ($v = 0.119 \text{ nm}^3$) and PS ($v = 0.095 \text{ nm}^3$) may be attributed mainly to their different glass transition temperatures of $T_g = 0^\circ \text{C}$ (PP) and $T_g = 95^\circ \text{C}$ (PS).

The intensity of the *o*-Ps component, I_3 , the average positron lifetime τ_{av} , the curve-shape parameter S and the peak height H of the DB spectra increase almost linearly

with the PS concentration. This is attributed to a linear superposition of the Ps yields of PP and PS in the PP–PS alloy.

After immersing PP into styrene monomer liquid, the annihilation parameters τ_3 , I_3 , and τ_{av} increase distinctly compared to those of pure PP, or of the PP–PS alloy with the same styrene weight fraction (27%). The effect is attributed to plasticisation of PP and can be used for in situ studies of the post-polymerisation process of styrene in solid PP.

The DBAR spectra may be fitted by a sum of three equi-centred Gaussian distributions. The width and intensity of the narrowest Gaussian correlates well with the behaviour of τ_3 and I_3 . From this it is concluded that it represents the narrow component being due to the *p*-Ps self-annihilation from holes in the amorphous phase.

After subtracting the narrowest Gaussian from the total DB curve, a broad component is obtained which represents the free positron and Ps pick-off annihilation with electrons bound to molecules. It represents the momentum distribution of bound electrons and is therefore sensitive to the chemistry of the polymeric material. In contrast to the other annihilation parameters, the normalised peak height H_b of this broad component does not show any change in the alloy range. This reflects the fact that the PP–PS alloy contains only hydrogen and carbon atoms in their units and gives evidence that H_b shows little or no correlation to Ps yield and the spatial structures of the free-volume holes. In POM and PTFE, for example, a strong decrease of H_b compared with hydrocarbon polymers is observed.

Acknowledgements

The authors are grateful to Th. Taplick/Merseburg for supplying the PP–PS alloy samples and to P. Hautajarvi/Helsinki, M. Eldrup/Riso and A. Shukla/Geneva for providing the programs LIFSPECFIT, SPARAM, PATFIT and MELT. Financial support from the EPSRC, UK is gratefully acknowledged. G.D. would like to thank the Benjamin Meaker Foundation (University of Bristol) for the award of the foundation's visiting professorship.

References

- [1] Utracki L. Polymer alloys and blends. Munich: Hanser Publisher, 1989.

- [2] Pluta M, Milczarek P, Wlochowicz A, Krystzewski M. Acta Polym 1991;42:485.
- [3] Rätzsch M, Bucka H, Hesse A, Arnold M, Borsig E. Proceedings of the conference on polymerwerkstoffe'96, September. Merseburg, Germany: Martin-Luther Universität Halle-Wittenberg, 1996 p. 152.
- [4] Mogensen OE. Positron annihilation in chemistry. Heidelberg: Springer, 1995.
- [5] Eldrup M, Lightbody D, Sherwood JN. Chem Phys 1981;63:51.
- [6] Nakanishi H, Jean YC. In: Schrader DM, Jean YC, editors. Positron and positronium chemistry, studies in physical and theoretical chemistry, vol. 57. Amsterdam: Elsevier, 1988. p. 159.
- [7] Jean YC. Microchem J 1990;42:72.
- [8] Jean YC. Positron annihilation. Proceedings of the 10th international conference. He Y-J, Cao B-S, Jean YC, editors. Mater Sci Forum 1995;59:175–8.
- [9] Pethrick RA. Progr Polym Sci 1997;22:1.
- [10] Goldstein M, Simha R. The glass transition and the nature of the glassy state. New York: New York Academy of Science, 1976.
- [11] Dlubek G, Saarinen K, Fretwell HM. Nucl Instr Meth Phys Res B 1998;142:139.
- [12] Dlubek G, Fretwell H, Alam MA. Macromolecules 2000;33:187.
- [13] LIFSPECFIT 5.1, Lifetime spectrum fit version 5.1. Technical University of Helsinki, 1992.
- [14] Shukla A, Peter M, Hoffmann L. Nucl Instr Meth A 1993;335:310.
- [15] Kirkegaard P, Pedersen NJ, Eldrup M. PATFIT-88. Report RISO-M-2740, 1989.
- [16] SPARAM, Laboratory of Physics, Technical University of Helsinki, 1992.
- [17] Okho Y, Uedono A, Ujihira Y. J Polym Sci Part B: Polym Phys 1995;33:1183.
- [18] Jean YC, Deng Q. J Polym Sci Part B: Polym Phys 1992;30:1359.
- [19] Stewens JR, Mao AC. J Appl Phys 1970;41:4273.
- [20] Kluin JE, Faupel F. Positron annihilation. Proceedings of the ninth international conference. Kajcsos Z, Szeles C, editors. Mater Sci Forum 1992;105–10:1613.
- [21] Hristov HA, Bolan B, Yee AF, Xie I, Gidley DW. Macromolecules 1996;29:8507.
- [22] Ban M, Kyoto M, Uedono A, Kawan T, Tanigawa S. J Polym Sci Part B: Polym Phys 1996;34:1189.
- [23] Yu Z, Yashi U, McGervey JD, Jamieson AM, Shima R. J Polym Sci B: Polym Phys 1994;32:2637.
- [24] Lightbody D, Sherwood JN, Eldrup M. Chem Phys 1985;93:475.
- [25] Dlubek G, Saarinen K, Fretwell HM. J Polym Sci B: Polym Phys 1998;36:1513.
- [26] Serna J, Abbe JCh, Duplatre G. Phys Stat Sol (a) 1989;115:389.
- [27] Reiter G, Kindl P. Phys Stat Sol (a) 1990;118:161.
- [28] Kindl P, Puff W, Sormann H. Phys Stat Sol (a) 1980(58):489.
- [29] Hirata K, Kobayashi Y, Ujihira Y. J Chem Soc Faraday Trans 1996;92:985.